

X-ray Crystal Structures of Cp*Ni(PEt₃)X [X = Br, O(*p*-C₆H₄Me), NH(*p*-C₆H₄Me), S(*p*-C₆H₄Me), OCH₃, CH₂C₆H₅, Me, H, PEt₃⁺]. Understanding Distortions and Trans Influences in Cyclopentadienyl Complexes

Patrick L. Holland, Michael E. Smith, Richard A. Andersen,* and Robert G. Bergman

Contribution from the Department of Chemistry, University of California, Berkeley, California 94720

Received June 4, 1997[⊗]

Abstract: The syntheses of Cp*Ni(PEt₃)Me and Cp*Ni(PEt₃)Br have been accomplished, starting from the useful starting material Cp*Ni(PEt₃)(acac). The X-ray crystal structures of Cp*Ni(PEt₃)X (X = Br, O(*p*-C₆H₄Me), NH(*p*-C₆H₄Me), S(*p*-C₆H₄Me), OCH₃, Me, CH₂Ph, H, PEt₃⁺) have been determined, providing a large sample of similar structures for the analysis of ring distortions as well as a systematic variation of X in order to evaluate the trans influence felt by opposite sides of the cyclopentadienyl ring. Major advances include demonstration that Cp can reduce its electron donation to a metal *without* “slipping”, the rational analysis of cyclopentadienyl distortions, and a well-supported trans-influence series for cyclopentadienylmetal complexes. In sum, d⁸ Cp*NiL₂ complexes are similar to d⁸ NiL₄ square-planar complexes in terms of bond lengths, binding geometry, and trans influences.

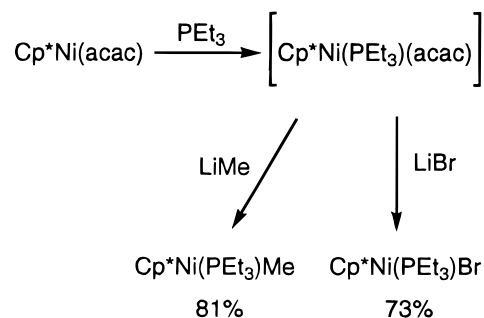
Introduction

Trans influences describe the effect of the trans ligand on the structural and ground-state properties of a ligand. They have been examined most thoroughly for square-planar and octahedral complexes, because in these cases, it is simple to define the ligand trans to a given ligand.¹ In cyclopentadienylmetal complexes, although some position of the “ring” may be trans to a ligand, that position in the ring may not be occupied by a carbon atom, complicating the analysis of trans influences using static methods like X-ray crystallography. One might hope to overcome this difficulty through the analysis of structures having only two non-Cp ligands and small, systematic variations of one ligand.

In this report we describe the X-ray crystal structures of Cp*Ni(PEt₃)X (**1-X**) (Cp* = pentamethylcyclopentadienyl; X = Br (**1-Br**), O(*p*-C₆H₄Me) (**1-OTol**), NH(*p*-C₆H₄Me) (**1-NHTol**), S(*p*-C₆H₄Me) (**1-STol**), OCH₃ (**1-OMe**), Me (**1-Me**) CH₂Ph (**1-Bn**), H (**1-H**)), and attempt to analyze trans influences on equivalent sides of the cyclopentadienyl ring.

In a recent contribution, a molecular-orbital model for the bonding in the isomorphous complexes Cp*M(acac) (M = Co, Ni; acac = acetylacetonate) was advanced.² This model elucidated the causes of a substantial “ene-allyl” distortion of the cyclopentadienyl ring in the crystal structure of Cp*Ni(acac). The crystal structures reported here demonstrate that the same model can be extended to explain distortions of the cyclopentadienyl ring in other d⁸ Cp*NiL₂ complexes, including new kinds of distortions. This systematic set of structures makes it possible both to assert with confidence that these relatively small distortions are significant and to define a trans-influence series in these pentamethylcyclopentadienylnickel complexes. In this way, the structural relationships between classic inorganic square-planar complexes and organometallic cyclopentadienyl compounds are explored.

Scheme 1



Results

Syntheses of Methyl and Bromide Complexes. Yamazaki and Mise reported that Cp*Ni(PR₃)I reacts with MeLi to produce Cp*Ni(PR₃)Me (R = Ph) and with LiCCPh to make Cp*Ni(PR₃)CCPh (R = Me).³ However, these reactions proceeded in low yield (34% and 36%, respectively), and the substitution reactions apparently failed for the chloride and bromide analogues. The reaction shown in Scheme 1 is a much more practical entry into the alkyl complex Cp*Ni(PEt₃)Me (**1-Me**). Treatment of Cp*Ni(acac)(PEt₃)² with a solution of methyl-lithium in diethyl ether (prepared from methyl chloride and lithium metal)⁴ gave a green solution of **1-Me** from which green crystals could be easily and reproducibly obtained in yields in excess of 80%.

The synthesis of Cp*Ni(PEt₃)Br (**1-Br**) may be accomplished from reaction of triethylphosphine with the bromide dimer [Cp*Ni(μ-Br)]₂,⁵ in a yield of 67%. An alternate synthesis was

(3) Mise, T.; Yamazaki, H. *J. Organomet. Chem.* **1979**, *164*, 391.

(4) Use of commercial methyllithium (Aldrich) gave substantial amounts of halide impurities Cp*Ni(PEt₃)X (X = Br, Cl), which presumably originated from LiX impurities in the methyllithium. (See: Lusch, M. J.; Phillips, W. V.; Sieloff, R. F.; Nomura, G. S.; House, H. O. *Org. Synth.* **1984**, *62*, 101.) However, if the commercial methyllithium was treated with dried 1,4-dioxane and subsequently filtered, this halide-free MeLi gave **1-Me** with halide content <2% by ¹H NMR spectroscopy.

[⊗] Abstract published in *Advance ACS Abstracts*, December 15, 1997.

(1) Appleton, T. G.; Clark, H. C.; Manzer, L. E. *Coord. Chem. Rev.* **1973**, *10*, 335.

(2) Smith, M. E.; Andersen, R. A. *J. Am. Chem. Soc.* **1996**, *118*, 11119.

Table 1. Crystal and Data Parameters for Structures on the CAD4 System

compound	1-Br	1-Me	compound	1-Br	1-Me
crystal dimensions (mm)	0.25 × 0.45 × 0.50	0.35 × 0.34 × 0.29	2θ range (deg)	3–50	3–50
<i>a</i> , <i>b</i> (Å)	14.416(2)	14.455(4)	reflections	1858	3638
<i>c</i> (Å)	8.727(1)	8.706(2)	unique reflections	1842	1814
<i>V</i> (Å ³)	1813.7(9)	1819.1(6)	<i>T</i> _{min} / <i>T</i> _{max}	0.75	0.84
space group	P4 (#81)	P4 (#81)	no. variables	172	162
<i>Z</i>	4	4	no. observations	1610	1594
<i>μ</i> _{calc} (Mo Kα, cm ⁻¹)	33.3	11.5	(<i>I</i> > 3σ(<i>I</i>))		
<i>d</i> _{calc} (g/cm ³)	1.46	1.19	<i>R</i> ; <i>R</i> _w	0.034, 0.039	0.085, 0.107
<i>T</i> (°C)	-112	-89	<i>R</i> (including zeros)	0.042	0.095
scan type	θ-2θ	θ-2θ	goodness of fit	1.36	3.25
reflections measured	+ <i>h</i> , + <i>k</i> , + <i>l</i>	+ <i>h</i> , + <i>k</i> , + <i>l</i>			

Table 2. Crystal and Data Parameters for Structures on the CCD/Area Detector System

compound	1-OTol	1-STol	1-OMe	1-Bn	1-H	P
crystal dimensions (mm)	0.50 × 0.40 × 0.18	0.18 × 0.30 × 0.51	0.08 × 0.21 × 0.23	0.35 × 0.35 × 0.15	0.49 × 0.35 × 0.25	0.25 × 0.20 × 0.10
<i>a</i> (Å)	16.5275(1)	16.7328(7)	14.6197(3)	16.9962(5)	8.7721(3)	9.5082(2)
<i>b</i> (Å)	12.6343(1)	16.9327(7)	8.7185(2)	15.6366(4)	13.6384(4)	17.9112(3)
<i>c</i> (Å)	11.0106(2)	16.6479(7)	29.0357(6)	16.5887(4)	14.8697(4)	16.8735(3)
β (deg)	90	91.703(1)	93.113(1)	94.441(1)	103.488(1)	100.857(1)
<i>V</i> (Å ³)	2299.16(4)	4714.8(3)	3695.5(1)	4395.4(2)	1729.91(8)	2822.18(8)
space group	<i>Pna</i> 2 ₁ (no. 33)	<i>P</i> 2 ₁ / <i>c</i> (no. 14)	<i>P</i> 2 ₁ / <i>c</i> (no. 13)	<i>P</i> 2 ₁ / <i>c</i> (no. 14)	<i>P</i> 2 ₁ / <i>c</i> (no. 14)	<i>P</i> 2 ₁ / <i>n</i> (no. 14)
<i>Z</i>	4	8	8	8	4	4
<i>μ</i> _{calc} (Mo Kα, cm ⁻¹)	9.22	9.84	11.3	9.59	12.0	9.2
<i>d</i> _{calc} (g/cm ³)	1.21	1.21	1.23	1.22	1.20	1.33
<i>T</i> (°C)	-150	-140	-104	-146	-114	-126
reflections	9312	19211	15486	17851	6994	11697
unique reflections	3555	7002	5687	6562	2584	4192
<i>T</i> _{min} / <i>T</i> _{max}	0.89	0.79	0.88	0.81	0.83	<i>a</i>
no. observations	3097	5524	4084	4493	2179	3118
(<i>I</i> > 3σ(<i>I</i>))						
no. variables	235	766	559	653	288	298
<i>R</i> ; <i>R</i> _w	0.024, 0.033	0.032, 0.041	0.030, 0.039	0.032, 0.042	0.023, 0.035	0.034, 0.050
<i>R</i> (including zeros)	0.025	0.042	0.044	0.049	0.026	0.073
goodness of fit	1.54	1.88	1.67	1.40	1.71	2.25

^a No absorption correction was applied.

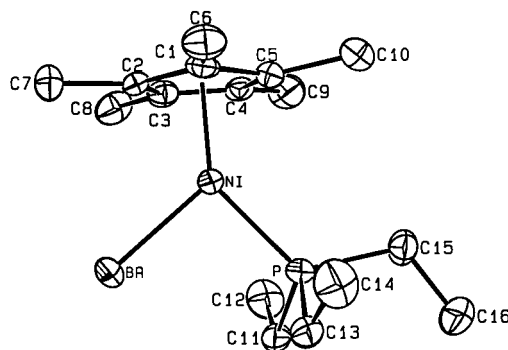
devised on the basis of the observation that LiX (X = Br, Cl) impurities in methyl lithium react with Cp*Ni(PEt₃)(acac) to form the corresponding Cp*Ni(PEt₃)X species. The metathesis reaction of Cp*Ni(PEt₃)(acac) with LiBr results in the formation of **1-Br** in high purity and yield (Scheme 1). This is the preferred synthesis for **1-Br**, as [Cp*Ni(μ-Br)]₂ is difficult to purify.⁵ Each of these syntheses demonstrate the utility of the 20-electron complex Cp*Ni(PEt₃)(acac)² as a synthon for Cp*Ni(PEt₃)X complexes.

X-ray Crystallography. All of the neutral complexes of the type Cp*Ni(PEt₃)X which we have synthesized (with the exception of X = OTf) are quite pentane-soluble, and cooling pentane solutions of these compounds provided single crystals for X-ray diffraction studies. Hence, a series of compounds with controlled variation were available for a systematic structural study. In the accompanying paper, the synthesis and solution behavior of these complexes are discussed.⁶

The structures of **1-Br**, **1-Me**, and **1-NHTol** were determined using a CAD4 diffractometer and the MOLEN structure solution package. All others were done on a Siemens SMART/CCD system, using SAINT and teXsan for integration and solution, respectively. Crystal and data parameters for the crystal structure determinations may be found in Tables 1 and 2. Selected bond distances may be found in Tables 3–6; full tabulations of data have been included as Supporting Information.

(5) Külle, U.; Fuss, B.; Khouzami, F.; Gersdorf, J. *J. Organomet. Chem.* **1985**, 290, 77.

(6) Holland, P. L.; Andersen, R. A.; Bergman, R. G. *J. Am. Chem. Soc.* **1997**, 119, 12800. Crystallographic details and an ORTEP diagram of **1-NHTol** may be found there.

**Figure 1.** ORTEP diagram of **1-Br**, using 50% probability ellipsoids.

The structure of the bromide complex **1-Br** was refined in space group *P*4; an ORTEP diagram of this structure is shown in Figure 1. This diagram demonstrates geometric features common to all of the structures in this paper. The Cp* ring is perpendicular to the plane defined by the Ni, P, and X atoms. The triethylphosphine ligand adopts a conformation in which the ethyl groups nearest the X atom are bent away from X, and the ethyl group away from X is bent away from the Cp* ligand.^{7,8} In **1-Br**, the Ni–Br distance is 2.335(1) Å, which is in the normal range for 4-coordinate nickel bromide complexes, but is extremely (~0.2 Å) short for a 5- or 6-coordinate nickel atom bound to bromide.⁹

(7) Stahl, L.; Ernst, R. D. *J. Am. Chem. Soc.* **1987**, 109, 5673.

(8) Stahl, L.; Trakernpruk, W.; Freeman, J. W.; Arif, A. M.; Ernst, R. D. *Inorg. Chem.* **1995**, 34, 1810.

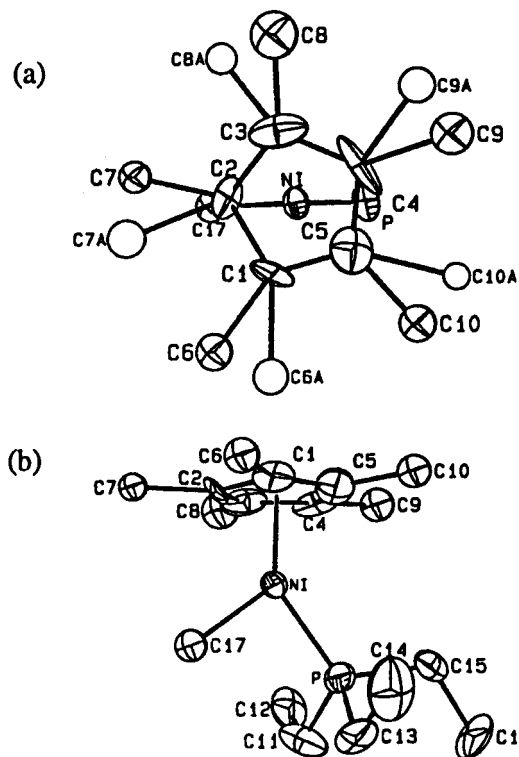


Figure 2. (a) Disorder model of **1-Me**; lower occupancy sites have "a" in the atom label and (b) ORTEP diagram of **1-Me**, using 50% probability ellipsoids. Only the higher occupancy atoms in the disorder model are shown.

Complex **1-Me** crystallizes in the same space group as **1-Br** ($P4$), but suffers from disorder across a crystallographic pseudo-mirror plane. Attempts to model the disorder as a twinned crystal were unsuccessful. Instead, the pentamethylcyclopentadienyl ring was modeled by treating the methyl groups as two partial-occupancy carbons (relative populations of 2:1, with the lower occupancy sites denoted by an "a" in the label). The disorder model is shown in Figure 2a. The pseudo-mirror plane contains the nickel and phosphorus atoms, C2, C15, C16, and C17. The inaccuracy of the structure precludes detailed discussion of the bond distances and angles, but it is possible to validate the significance of some geometrical features of **1-Me** by comparison with the other structures reported here.

In the structure of **1-NHTol**, there were two crystallographically independent molecules in the asymmetric unit, but the general geometric features of the two molecules are the same.⁶ Each NH proton was located in a Fourier electron density difference map: their positions indicate that the geometry about each nitrogen atom is planar, presumably due to delocalization of the electrons in the nitrogen p orbitals into the π systems of the phenyl rings.¹⁰

The structures of **1-STol** and **1-Bn**, like that of **1-NHTol**, each have two independent molecules in the asymmetric unit. This offered the opportunity to gain information about the reproducibility of metrical data in the presence of different intermolecular forces. In **1-NHTol** and **1-STol**, all of the bond lengths are duplicated to within 0.01 Å, and bond angles to within 3°; in **1-Bn**, the only metrical parameter for which these limits did not hold was the Ni–C distance, which varies by

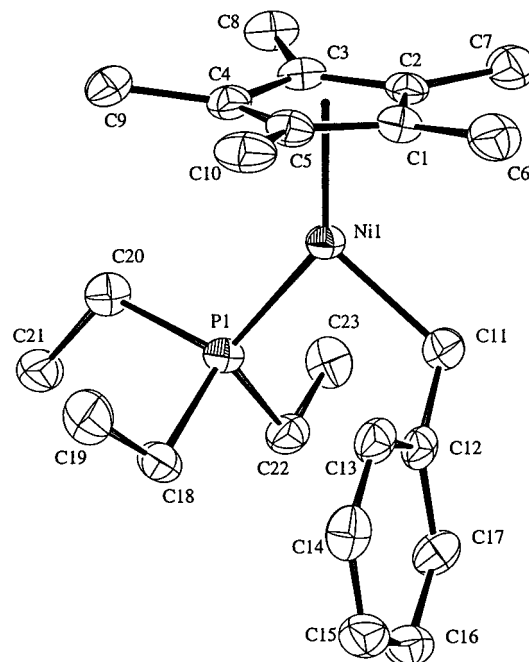


Figure 3. ORTEP diagram of one molecule of **1-Bn**, using 50% probability ellipsoids.

0.03 Å between the two independent molecules (see Table 6). Importantly, the differences between the P–Ni–N–C, P–Ni–S–C and P–Ni–C–C dihedral angles in the two chemically identical but crystallographically independent molecules in the structures of **1-NHTol**, **1-STol**, and **1-Bn**, respectively, are less than 15°. This suggests that electronic and crystal packing effects are minor in determining the geometry of the X ligands in the crystal structures.

Each nickel–sulfur distance in **1-STol** is 2.20 Å; this is long compared to Ni–S bonds in square planar compounds (~2.15 Å), but short for a 5-, 6-, or 7-coordinate nickel atom, in which Ni–S distances usually lie between 2.3 and 2.4 Å.⁹ The Ni–C bond in **1-Bn** is harder to compare to a "typical" Ni–C bond, because few alkylnickel complexes have been crystallographically characterized,⁹ but the distances of 1.979(3) Å and 2.007(4) Å compare favorably to that in **1-Me** (1.96(1) Å).

Unlike its nitrogen, sulfur, and carbon analogues, **1-OTol** crystallized in the space group $Pna2_1$, but the molecular geometric parameters were similar to those of its congeners. The nickel–oxygen distance is 1.889(2) Å; this distance is reasonable for a 4-coordinate complex (these typically lie in the range 1.84–1.89 Å), but quite short for a molecule with a coordination number of 5 or greater (these are typically between 1.98 and 2.02 Å).⁹ An ORTEP diagram of **1-Bn** is displayed in Figure 3; ORTEP diagrams of **1-OTol** and **1-STol** are in the Supporting Information.

The hydride ligand in complex **1-H** is drastically different in size from the other X ligands, and it crystallizes in a different space group, $P2_1/c$, with only one molecule in the asymmetric unit. This structure was extremely well-behaved, and it was possible to refine all of the hydrogen atoms in the model with isotropic thermal parameters, giving a Ni–H distance of 1.46(3) Å.¹¹ Very few Ni–H bond distances have been determined accurately by X-ray crystallography; compared to the others that are known, this distance is not unreasonable.^{12–14} Due to the smaller size of the hydride ligand, the X–Ni–L (L = Cp

(9) Cambridge Structural Database: Allen, F. H.; Davies, J. E.; Galloy, J. J.; Johnson, O.; Kennard, O.; Macrae, C. F.; Mitchell, E. M.; Mitchell, G. F.; Smith, J. M.; Watson, D. G. *J. Chem. Inf. Comput. Sci.* **1991**, *31*, 187.

(10) Villanueva, L. A.; Abboud, K. A.; Boncella, J. M. *Organometallics* **1994**, *13*, 3921.

(11) An ORTEP diagram of **1-H** may be found in the Supporting Information.

(12) Müller, U.; Keim, W.; Krüger, C.; Betz, P. *Angew. Chem., Int. Ed. Engl.* **1989**, *28*, 1011.

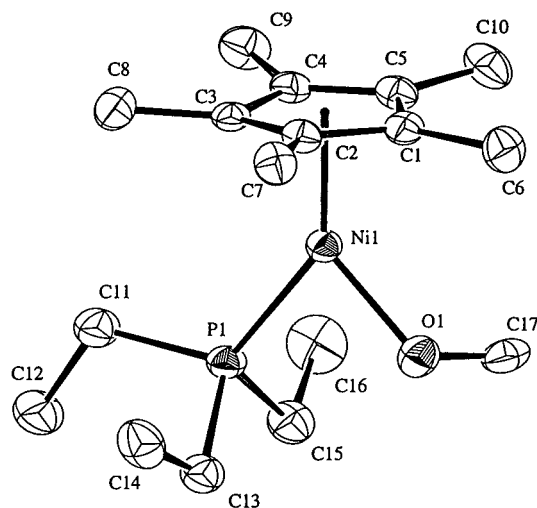


Figure 4. ORTEP diagram of one molecule of **1-OMe**, using 50% probability ellipsoids.

centroid, PEt_3 angles are smaller than those found in the complexes with more sterically demanding X ligands (Table 6).

The methoxide complex **1-OMe** crystallized in space group $P2_1/c$, with two molecules in each asymmetric unit. An ORTEP diagram of one is shown in Figure 4. This constitutes the first structurally characterized monomeric nickel methoxide complex. The Ni–O distances in **1-OMe** are 1.877(2) and 1.880(2) Å; these distances are not significantly different from the Ni–O distance in **1-OTol**. Unfortunately, refinement led to a model in which the carbon atom in each methoxide ligand had a somewhat large RMS amplitude in a direction skew to the C–O bond. However, B_{equiv} was not high for these atoms. Because of this crystallographic abnormality, the C–O bond parameters have a large uncertainty.

A cationic product with two triethylphosphine ligands, $\text{Cp}^*\text{Ni}(\text{PEt}_3)_2^+ \text{OTf}^-$ (**1-PEt₃**), crystallized from a THF–ether solution to give a crystal for which the structure was solved in space group $P2_1/c$. An ORTEP diagram of **1-PEt₃** is shown in Figure 5. Interestingly, one phosphine group (P(2)) has the conformation seen in all of the other crystal structures, but the other phosphine (P(1)) sits with one ethyl group away from the Cp^* ring and two parallel to it. This suggests some “gearing” of the phosphine ligands in this sterically crowded complex. The Ni–P distances are nearly equivalent (2.198(1) and 2.203(1) Å), and significantly longer than the Ni–P distances in the other compounds; this is also attributable to steric effects. In solution NMR spectra, the phosphine ligands are equivalent; the ethyl groups are undoubtedly dynamic outside the restriction of the crystal lattice.

Discussion

Cyclopentadienyl Ring Distortions. Distortions of the cyclopentadienyl rings are observed in all of the $\text{Cp}^*\text{Ni}(\text{PEt}_3)\text{X}$ structures determined here. Most of them fall into two categories (the others will be addressed later).

(1) Ene-allyl. Several structures show a distortion of the cyclopentadienyl ring in which two adjacent C–C bonds are short, and the C–C bond opposite these two bonds is even shorter, near the length expected for a double bond. Carbon–

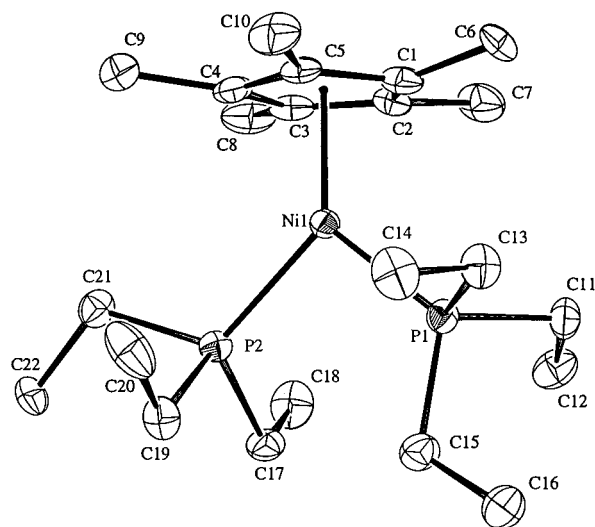


Figure 5. ORTEP diagram of **1-PEt₃**, using 50% probability ellipsoids.

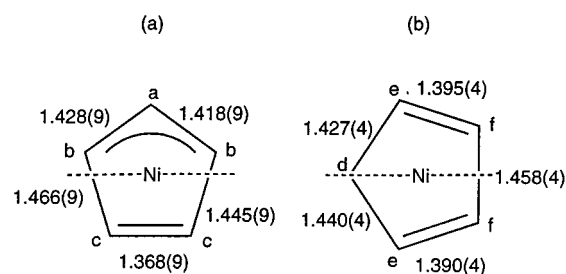


Figure 6. (a) Ene-allyl distortion in **1-Br** and (b) diene distortion in one molecule of **1-STol**. In each case, the Ni–P–X plane is indicated by a dashed line. Distances are in angstroms.

Table 3. Ene-Allyl Distortions: C–C Bond Lengths (Å)^a

	C _c –C _c	C _a –C _b	C _b –C _c
1-Br	1.368(9)	1.418(9)	1.445(9)
		1.428(9)	1.466(9)
1-NHTol (no. 1)	1.390(8)	1.417(8)	1.452(8)
		1.419(8)	1.464(8)
1-Bn (no. 1)	1.407(5)	1.417(5)	1.446(5)
		1.418(5)	1.451(5)
1-Bn (no. 2)	1.409(5)	1.418(5)	1.443(5)
		1.423(5)	1.448(5)
1-H	1.406(3)	1.428(3)	1.437(3)
		1.422(3)	1.445(3)
1-OMe (no. 2)	1.399(5)	1.421(5)	1.440(5)
		1.429(5)	1.449(5)

^a C_a, C_b, C_c defined in Figure 6.

carbon bond distances in the structures showing this kind of “ene-allyl” distortion are given in Table 3, and this distortion is illustrated in Figure 6a, with the bond lengths from the structure of **1-Br** shown as an example. In this case, the distortion is highly significant, with C–C distances within the ring varying over a range of 0.1 Å, but in the case of **1-H**, the range is only 0.04 Å. In Tables 3–6, we have defined ene-allyl distortions as those in which two adjacent short C–C bonds have lengths which differ by 0.010 Å or less.

(2) Diene. In other structures, the cyclopentadienyl ring has two nonadjacent, equally short C–C bonds. The values in Table 4 show that the ranges of C–C bond lengths in this “diene” distortion are generally smaller than in the ene-allyl distortions shown above. An example is in the structure of **1-STol**, where one of the molecules in the asymmetric unit has the ring C–C bond distances shown in Figure 6b. Diene distortions have been defined as those in which there are two nonadjacent ring C–C distances of 1.40 Å or less.

(13) Saito, T.; Nakajima, M.; Kobayashi, A.; Sasaki, Y. *J. Chem. Soc., Dalton Trans.* **1978**, 482.

(14) Sacconi, L.; Orlandini, A.; Midollini, S. *Inorg. Chem.* **1974**, *13*, 2850.

Table 4. Diene Distortions: C–C Bond Lengths (Å)^a

	C _f –C _f	C _e –C _f	C _d –C _e
1-NHTol (no. 2)	1.440(8)	1.389(8)	1.451(8)
		1.394(8)	1.457(8)
1-STol (no. 1)	1.458(4)	1.390(4)	1.427(4)
		1.395(4)	1.440(4)
1-PEt₃	1.471(5)	1.364(5)	1.440(5)
		1.395(5)	1.461(5)
1-OTol	1.464(3)	1.386(4)	1.437(4)
		1.402(4)	1.454(4)

^a C_d, C_e, C_f defined in Figure 6.

It is common to picture an ene-allyl-distorted ring as an η^3 -bound ligand with a partially coordinated double bond, and a diene-distorted ring as an η^1 -bound ligand with two partially coordinated double bonds. However, treating the Cp* ligands in the complexes here as “slipped” is clearly *not* valid: in each of these structures, all of the Ni–C(ring) distances are within 0.1 Å of each other. *None of these structures has a slipped cyclopentadienyl ring.*¹⁵

Interestingly, the type of distortion is correlated with the orientation of the carbon atoms of the ring with respect to the plane containing the Ni, P, and X atoms. The limiting orientations are demonstrated in Figure 6. In Figure 6a, the two carbon atoms closest to the NiPX plane (C_b) are equidistant from that plane. In Figure 6b, one carbon (C_d) is *in* the plane of the NiPX fragment.¹⁶ In Table 6, the positions of the rings in the crystal structures are characterized by the distance of the nearest Cp ring carbon to the NiPX plane. In each structure with a carbon atom “on” (less than 0.10 Å) the NiPX plane, the Cp ring has a diene distortion, while in each one with a carbon atom “off” (greater than 0.20 Å) the NiPX plane, the Cp ring shows an ene-allyl distortion. In each case, the NiPX plane and the distortion are oriented as shown in Figure 6, with the short bonds *off* the NiPX plane.

The electronic reasons for both ene-allyl and diene distortions have been analyzed theoretically. Dahl and co-workers first discussed the ene-allyl distortion of a Cp ring in the compound CpNi(C₅H₅C₂(CO₂CH₃)₂);¹⁷ additional discussions may also be found in the contexts of Cp*Co(CO)₂¹⁸ and Cp*Ni(acac).² Werner and Hofmann have independently discussed a diene distortion in (η^5 -Cp)Pd(PⁱPr₃)(η^1 -Cp), along with calculations on the model compound (η^5 -Cp)Pd(PH₃)CH₃.¹⁹ The explanations of the distortions are essentially identical and they can be summarized as follows (“plane” always refers to the NiPX plane). Of the two π -symmetry interactions between the metal and the cyclopentadienyl fragment, the out-of-plane (b₁ symmetry) bonding *and* antibonding orbitals are filled, while the in-plane (b₂ symmetry) bonding orbital (but *not* the antibonding orbital) is occupied (Figure 7).²⁰ Thus, net metal-Cp bonding occurs in-plane, but not in the out-of-plane regions. The differential population of these two orbitals results in C=C π -bond localization in the out-of-plane regions of the Cp ring.

This electronic situation is manifested as an ene-allyl distortion

(15) For a review on “slipped” cyclopentadienyl rings, see: O'Connor, J. M.; Casey, C. P. *Chem. Rev.* **1987**, *87*, 307.

(16) In a recent paper, these distortions are referred to as “staggered” and “eclipsed”, respectively: Cross, R. J.; Hoyle, R. W.; Kennedy, A. R.; Manojlovic-Muir, L.; Muir, K. W. *J. Organomet. Chem.* **1994**, *468*, 265. In this paper, a CpPd(X)(L) complex was found to have a distortion of the type we call “intermediate”, and this (combined with an analysis of several previously characterized Cp*Pd(X)(L) complexes) led Cross *et al.* to use many of the same arguments found here. However, we can draw firmer conclusions because (a) the Cp* ligand is less prone to librational motion, and (b) this paper lists a larger range of similar complexes.

(17) Dahl, L. F.; Wei, C. H. *Inorg. Chem.* **1963**, *2*, 713.

(18) Byers, L. R.; Dahl, L. F. *Inorg. Chem.* **1980**, *19*, 277.

(19) Werner, H.; Kraus, H.-J.; Schubert, U.; Ackermann, K.; Hofmann, P. *J. Organomet. Chem.* **1983**, *250*, 517.

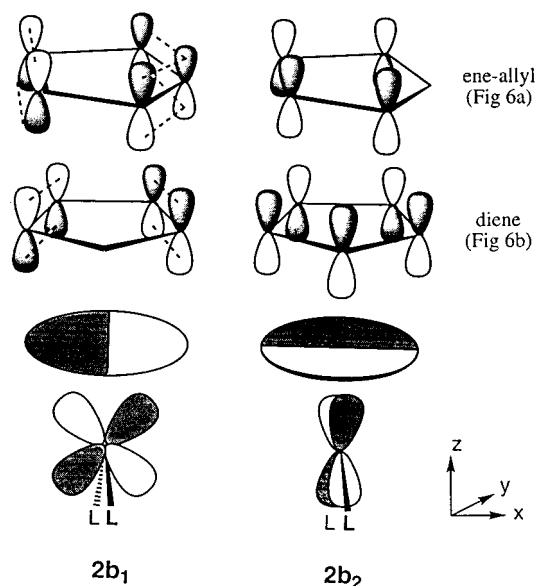


Figure 7. Representations of the HOMO (2b₁) and LUMO (2b₂) in 18-electron molecules of the type CpML₂, with idealized C_{2v} symmetry,²⁰ and in the ene-allyl and diene geometries, demonstrating that each is M–Cp antibonding. The two ligands (in these cases, PEt₃ and X) lie above and below the plane of the paper along the y axis.

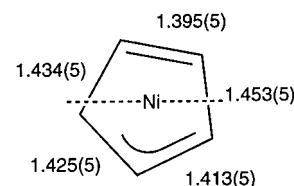


Figure 8. Intermediate distortion in one molecule of **1-OMe**. The Ni–P–O plane is indicated by a dashed line. Distances are in angstroms.

tion when the cyclopentadienyl carbon atoms are oriented as in Figure 6a, and as a diene distortion when the ring is rotated by just a few degrees. In Figure 7, the idealized “ring” is displayed in an orbital interaction diagram, along with diagrams showing carbon atoms in “ene-allyl” and “diene” positions. In other cases, such as **1-OMe**, the situation is intermediate between these extremes: neither the orientation nor the bond localization in the Cp ring (Figure 8) belong to either category, but the distortion observed remains consistent with the same orbital model. In these structures, the bonds farthest from the NiL₂ plane are shortest, and those that intersect it are the longest. Other examples of this intermediate situation are found in Table 5. Thus, distortions of the *same* symmetry are seen even when the Cp ring is not oriented “on” or “off” the NiL₂ plane.¹⁶

Ene-allyl distortions of cyclopentadienyl rings have sometimes been discussed in terms of the “fold angle”, which describes the angle between the least-squares C_a/C_b plane and the least-squares C_b/C_c plane (*i.e.*, the angle between the “alkene” and “allyl” portions of the ring, Figure 6a). In structures with ene-allyl distortions,² the ring folds away from the nickel in the “ene” and “allyl” parts of the ring, because less Ni–Cp bonding occurs there. This definition of the fold angle becomes troublesome when the ring has a diene distortion. In general, all of the rings in this study show a similar “saddle”

(20) In this discussion, the cyclopentadienyl ring is approximated as a circle and the ligands are identical, giving idealized C_{2v} symmetry; symmetry labels are given in this point group. In this way, we avoid the need to distinguish the C_s symmetry of Figure 6a (in which σ is vertical, and the HOMO and LUMO in Figure 7 are a' and a'', respectively) from the C_s symmetry of Figure 6b (in which σ is horizontal, and the HOMO and LUMO in Figure 7 are a'' and a', respectively).

Table 5. Intermediate Distortions: C–C Bond Lengths (Å)

	C(1)–C(2)	C(2)–C(3)	C(3)–C(4)	C(4)–C(5)	C(5)–C(1)
1-STol (no. 2)	1.422(4)	1.406(4)	1.436(4)	1.384(4)	1.458(4)
1-OMe (no. 1)	1.425(5)	1.413(5)	1.453(5)	1.395(5)	1.434(5)

Table 6. Trends in the Structural Parameters and Spectroscopy of Complexes of Cp*Ni(PEt₃)X

maxcolw;500q X	NHTol		STol		OMe		Bn		Me	H		
	OTol	Br	no. 1	no. 2	no. 1	no. 2	no. 1	no. 2				
Ni–P distance (Å)	2.1618(6)	2.160(2)	2.150(2)	2.144(2)	2.1499(9)	2.1544(8)	2.142(1)	2.139(1)	2.1357(9)	2.1392(9)	2.109(4)	2.0844(5)
Ni–X distance (Å)	1.889(2)	2.335(1)	1.903(5)	1.903(5)	2.2031(9)	2.1982(9)	1.877(2)	1.880(2)	1.979(3)	2.007(4)	1.96(1)	1.46(3)
Ni–Cp plane (Å)	1.75	1.76	1.76	1.76	1.77	1.76	1.76	1.75	1.78	1.79	1.76	1.73
Cp–Ni–X angle (deg)	125.4	127.7	126.9	126.3	125.0	125.9	132.3	131.8	128.0	126.3	129	130.1
Cp–Ni–P angle (deg)	140.7	139.6	140.0	142.1	141.1	139.6	141.3	141.5	139.3	138.7	141	147.1
P–Ni–X angle (deg)	92.99(5)	92.46(5)	92.9(2)	91.4(2)	93.54(3)	93.88(4)	86.26(8)	86.57(8)	92.6(1)	95.0(1)	90.2(4)	83(1)
P–Ni–E–C dihedral ^c (deg)	69.3(2)	N/A	74.8(5)	72.3(5)	68.5(1)	76.6(1)	108.2(3)	108.8(2)	63.1(2)	48.2(3)	N/A	N/A
“ene-allyl” (EA), “diene” (D), or intermediate (I)	D	EA	EA	D	D	I	I	EA	EA	EA	a	EA
nearest Cp carbon to Ni–P–X plane (Å)	0.04	0.23	0.34	0.16	0.05	0.12	0.20	0.23	0.30	0.27	a	0.22
Ni–C _{cp} (trans P) (Å)	2.118(2)	2.112(6)	2.133(6)	2.135(8) ^b	2.133(4) ^b	2.125(3)	2.098(3)	2.109(3)	2.116(3)	2.104(3)	a	2.059(2)
Ni–C _{cp} (trans X) (Å)	2.084(2)	2.084(6)	2.091(5)	2.101(6)	2.112(3)	2.093(3)	2.123(10) ^b	2.092(3)	2.149(3)	2.170(3)	a	2.117(2)
Δ(Ni–C _{cp}) (Å)	0.034(3)	0.028(8)	0.042(8)	0.034(10)	0.021(6)	0.032(4)	–0.025(11)	0.017(4)	–0.033(4)	–0.066(4)	a	–0.058(3)
³¹ P NMR (PEt ₃) (δ) ^d	21.8	24.5	25.1	25.1	25.0	25.0	23.8	23.8	29.4	29.4	34.9	38.0
¹ H NMR (Cp*) (δ) ^d	1.44	1.49	1.54	1.54	1.63	1.63	1.61	1.61	1.76	1.76	1.80	2.06

^a Disorder in the structure makes detailed Cp* ring parameters untrustworthy. ^b In cases where a Cp carbon is on the Ni–P–X plane, the average of the two opposite Ni–C distances is given. ^c “E” refers to the nickel-bound atom of the X ligand. ^d NMR spectra were obtained on C₆D₆ solutions.

shape with the carbon atoms nearest the NiPX plane closer to the nickel atom and the carbon atoms farthest from the NiPX plane more distant from the nickel atom, but the fold angles derived from these saddle-shaped distortions are only 4–6° in all cases. Thus, the approximation of the ring as flat for the purposes of qualitative discussions is justifiable; the distortion is not as pronounced as in Cp*Ni(acac) (fold angle = 9.3°).²

It is noteworthy that the areas of the rings having greater Ni–C bonding (inferred from the longer C–C distances in these regions, the slight folding of the rings, and the agreement with the orbital model above) are in the NiPX planes. Thus, the bonding in the molecules discussed here approximates square-planar geometry about nickel. This is consistent with the preference of Ni(II) for square-planar over tetrahedral geometry and with the diamagnetism of these Cp*Ni(PEt₃)X compounds.²¹ As mentioned above, this pseudo-square-planar geometry is not attained by “slipping” the cyclopentadienyl ring to η³-binding; the nickel atom simply “ignores” the out-of-plane regions of the ring with no movement of the Cp ring centroid. Our suggestion that the nickel atom is pseudo-square planar is supported by the Ni–X distances, which are more typical of 4-coordinate (16-electron) Ni(II) complexes than of 5- (18-electron) or 6-coordinate (20-electron) Ni(II) complexes. This reflects the low “effective” coordination number of the nickel atom.

Analysis of the structures reported here shows that the antibonding interactions in the model first proposed by Dahl not only cause ene-allyl distortions or diene distortions: a wider range of distortions can be explained by the selective occupancy of the two M–Cp antibonding molecular orbitals shown in Figure 7. Arranging the X ligands in a trans-influence order (Table 6) suggests that there is no electronic effect favoring either distortion. Likewise, in some cases (**1-NHTol**, **1-STol**), molecules with different distortions are found in a crystal of the same compound. These observations demonstrate that only “random”, low-energy effects like crystal packing determine the type of distortion in the cyclopentadienyl rings. Thus, even

though Hofmann’s theoretical results for an analogous palladium system indicated that a diene distortion should be favored because of favorable M–C_d bonding,¹⁹ this preference is extremely small, at least for the nickel compounds discussed here.²²

As a final note on this subject, a search⁹ of compounds of the type Cp*ML₂ (Cp* = C₅R₅, M = Co(I), Rh(I), Ir(I), Ni(II), Pd(II)) shows that each crystallographically well-characterized example of a d⁸ Cp*ML₂ compound shows a distortion of the type described here.^{6,23,24} This strongly suggests that the qualitative molecular-orbital arguments of Dahl are widely applicable. Notably, many examples were found of the diene and intermediate types as well as the ene-allyl type originally treated by Dahl.

Trans Influences in Cp*MLX Compounds. The previous discussion which likens the M–Cp bonding in d⁸ Cp*MLX complexes to square-planar coordination suggests that it should be possible to define a trans influence series similar to those established for square-planar complexes.¹ However, trans influences are very difficult to evaluate in individual cyclopentadienyl complexes, because the position in the cyclopentadienyl “ring” which is *trans* to a ligand may or may not be occupied by one of the carbon atoms of the cyclopentadienyl ligand. This problem can be overcome by examining a large number of similar crystal structures; the gradual changes between the several structures of the class Cp*Ni(PEt₃)X allow reasonable observations to be made about relative trans influences. In Table 6, the M–C distances are listed for the bonds most nearly opposite each ligand. In cases where two M–C bonds are equally close to being *trans* to a ligand, the average of these M–C bonds was used.

A potential problem with this method is that, when a diene distortion is present, the M–Cp bonding orbital (b₂ symmetry)

(22) This conclusion was also reached by Cross *et al.* for CpPd(X)(L) complexes. See ref 16.

(23) This generalization did not hold for complexes with ligands of indeterminate oxidation level (*e.g.*, catecholate), those with activating or chelating groups on the Cp ring, three-legged piano stools, or polymetallic complexes. This is due to changes in the orbitals at the metal which invalidate the explanation presented above.

(24) Holland, P. L.; Andersen, R. A.; Bergman, R. G. *J. Am. Chem. Soc.* **1996**, *118*, 1092.

(21) Cotton, F. A.; Wilkinson, G. *Advanced Inorganic Chemistry*, 5th ed.; John Wiley & Sons: New York, 1988; pp 746–748.

has a maximum at a carbon atom (C_d) on one side of the ring, but the maximum is *between* atoms (C_f) on the other side of the ring (see Figures 6 and 7). Thus, the M–C_d bond, being at the M–Cp bonding maximum, should be shorter than the two M–C_f bonds. In the crystal structure of **1-PEt₃**, the PEt₃ and X ligands are identical, and so the size of this effect on the Ni–C bond lengths can be evaluated without concern for the differential trans influences of PEt₃ and X. They differ by 0.016(6) Å, in the expected direction. Additionally, in **1-NHTol**, there is a diene distortion which can be compared to another molecule in the asymmetric unit in which the distortion is ene-allylic (in an ene-allyl distortion, both C_b's are equivalent with respect to the idealized b₁ and b₂ orbitals). In this case, too, the value for Δ(Ni–C) is smaller by about 0.01 Å in the molecule with the diene distortion. However, these effects are smaller than the 0.02–0.03 Å ranges of Δ(Ni–C) found in other molecules having two molecules in the asymmetric unit and the *same* kind of distortion. Thus, we conclude that the effect of the diene distortion on the Ni–C_d distance is probably less than random variation due to packing forces.

Table 6 shows that for complexes **1-Bn** and **1-H**, Ni–C (trans to X) is longer than Ni–C (trans to P), while for heteroatom ligands, Ni–C (trans to X) is shorter than Ni–C (trans to P). The only exception to this “rule” is the methoxide complex **1-OMe**, in which Ni–C (trans to X) is longer than Ni–C (trans to P). Unfortunately, these measurements are close enough to being statistically insignificant that finer distinctions cannot be discerned. The agreement between the several structures of each type, however, indicates that this general trend is meaningful. From these results, it can be concluded that the trans-influence order for Cp*NiL₂ is alkyl, hydride > phosphine > NHAr, OAr, SAR, Br; this agrees with commonly accepted trans-influence orders.¹

The methoxide ligand in **1-OMe** has an abnormally strong trans influence relative to the other oxygen, nitrogen, sulfur, and bromine ligands. In analogy to the preceding paper,⁶ this could be caused by π- or σ-symmetry interactions. On the basis of the conformations of the ligands above, the fact that the Ni–O distances are almost identical in **1-OMe** and **1-OTol**, and the implications of thermochemical studies in the accompanying paper, it seems most likely that the large trans influence of **1-OMe** is largely mediated by a difference in the Ni–O σ bonds and not by ππ/dπ repulsion. However, it is dangerous to draw strong conclusions from any one of the Δ(Ni–C) values by itself, in view of the uncertainty associated with these values.

An operational test of the trans influences in this series of complexes comes from the chemical shifts of the Cp* methyl and phosphine resonances in the ¹H and ³¹P NMR spectra of these complexes (Table 6). Although the use of chemical shifts to evaluate trans influences is questionable in many cases,²⁵ in this series there is a correlation (R = 0.93) between the ¹H chemical shift of the Cp* ligand and the ³¹P shift of the phosphine ligand (Figure 9), and these also follow a typical trans-influence series.¹ A plot of the chemical shift of the Cp* protons in the ¹H NMR spectrum vs Δ(Ni–C) is also shown in Figure 9, demonstrating a correlation (R = 0.81) between the crystallographic trans influence and the spectroscopic trans influence. This agreement is evidence that the easily obtained NMR shifts give useful qualitative information about trans influences in this system.

Another influence caused by X is a monotonic change in Ni–P distances (Table 6); this distance gradually decreases from 2.1618(6) Å in **1-OTol** to 2.0844(5) Å in **1-H**. Not surprisingly, the Ni–P distance also correlates with the ³¹P shift of the

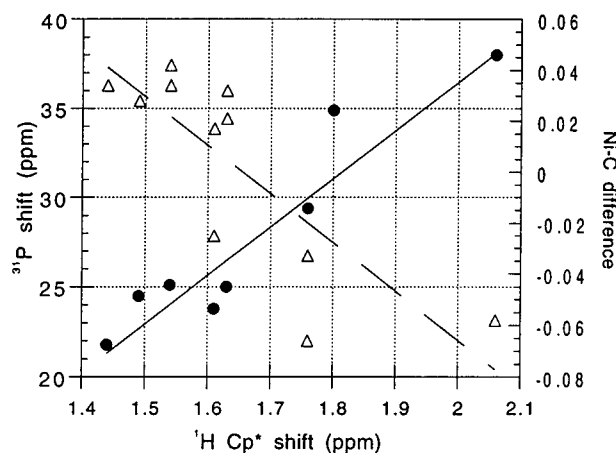


Figure 9. Correlations between the chemical shift of the Cp* resonance in the ¹H NMR spectrum, the chemical shift of the resonance in the ³¹P{¹H} NMR spectrum, and Δ(Ni–C_{Cp}) (as in Table 6). Phosphorus NMR shifts are shown as solid circles, and Δ(Ni–C_{Cp}) values are shown as triangles.

phosphine ligand (R = 0.93). The sources of cis influences are less understood than those for trans influences, and can arise from several sources.²⁶ The compounds with longer Ni–P bonds are also those which exchange phosphine ligands the most rapidly; in the preceding paper, we suggest that this ordering is associated with the thermodynamic preference for electrostatic or covalent bonding in different Cp*Ni(PEt₃)X complexes.⁶

Conclusions

Distortions of the cyclopentadienyl group are general to 18-electron Cp*ML₂ complexes (Cp' = substituted or unsubstituted cyclopentadienyl group).¹⁶ This general situation has been examined in detail for a series of complexes of the form Cp*Ni(PEt₃)X. These distortions invariably involve M–Cp bonding which approximates a square-planar geometry about the metal atom, with concomitant Cp ring C=C localization in the out-of-plane regions of the ring. The distortion may be expressed in a range of forms, including the symmetric ene-allyl and diene forms recognized previously. Thus, deviations of cyclopentadienyl ligands from 5-fold symmetry can be explained in terms of a simple qualitative molecular-orbital model.

This work also reveals a rational trans-influence order, as transmitted to the two sides of a cyclopentadienyl ligand: alkyl, hydride > phosphine, methoxide > arylamide, aryloxy, arylthiolate, bromide. This represents the extension of the useful concept of trans influences to the ubiquitous CpML_n class of organometallic compounds, and highlights their similarity to traditional square-planar complexes.

It is important to note that each of the effects shown here is on the edge of statistical significance, and the common practice of inferring distortional and trans-influence information from a single structural determination is questionable at best. In this report, though, the 12 independent molecular structures described *all* showed the same trends, and our conclusions are supported by the agreement with many other structures in the Cambridge Structural Database, as well as known trans-influence series.

Experimental Section

General. All manipulations were carried out under an atmosphere of dry nitrogen using standard Schlenk and dry box techniques. Details of instruments and techniques have been described.² LiBr was dried overnight *in vacuo* at 200 °C. Halide-free methyllithium was synthesized from literature procedures,⁴ allowing halides to settle for one week

(25) Appleton, T. G.; Bennett, M. A. *Inorg. Chem.* **1978**, *17*, 738.

(26) Hartley, F. R. *Chem. Soc. Rev.* **1973**, *2*, 163.

before filtering. Alternatively, commercial methyllithium could be freed from halides as follows. In the glovebox, 5 drops of 1,4-dioxane (distilled from Na/benzophenone) were added to ~10 mL of methyllithium solution ("1.4 M" in diethyl ether, fresh from Aldrich), causing a white powder to precipitate. The resulting suspension was allowed to settle, and the supernatant was filtered through a plug of dried Celite to give the "purified" solution. Aliquots of such solutions were titrated with 1,1-diphenylacetone *p*-tolylhydrazone (Aldrich); the solutions were typically 0.6–0.8 M in methyllithium after such treatment. The syntheses of many of the compounds may be found in the accompanying paper.⁶

Cp*Ni(PEt₃)Br (1-Br) from [Cp*Ni(μ-Br)]₂. To a solution of [Cp*Ni(μ-Br)]₂⁵ (0.27 g, 0.49 mmol) in CH₂Cl₂ (60 mL) at -20 °C was added PEt₃ (0.15 mL, 1.0 mmol). Upon mixing, the solution immediately changed color from red-brown to clear red. After the mixture was stirred at -20 °C for 3 h, the volatile materials were completely removed under reduced pressure and the residue was extracted with pentane (150 mL). The red solution was filtered and the filtrate was concentrated to ~60 mL. Cooling to -30 °C afforded red blocks. Concentration of the mother liquor provided an additional crop of crystals for a total yield of 0.26 g (0.66 mmol, 67%). Mp: 165–167 °C dec. IR: 2726 (w), 1532 (w), 1420 (s), 1346 (s), 1250 (m), 1240 (m), 1156 (m), 1066 (w), 1034 (s), 1022 (sh), 982 (w), 972 (w), 942 (w), 768 (s), 720 (s), 678 (m), 636 (m), 618 (w), 570 (w), 540 (w), 439 (m), 377 (m), 329 (w). ¹H NMR (C₆D₆): δ 1.49 (d, *J* = 1.5 Hz, 15H, C₅Me₅), 1.40 (d of q, *J* = 8.5, 7.5 Hz, 6H, CH₂CH₃), 0.93 (d of t, *J* = 16, 7.5 Hz, 9H, CH₂CH₃). ³¹P{¹H} NMR (C₆D₆): 24.53. EIMS: 390 (72,73); 391 (14,13); 392 (100,100); 393 (20,19); 394 (33,33); 395 (7,7); 396 (5,5). Anal. Calcd for C₁₆H₃₀NiBrP: C, 49.0; H, 7.71. Found: C, 48.9; H, 7.80.

Cp*Ni(PEt₃)Br (1-Br) from Cp*Ni(acac). To a solution of Cp*Ni(acac) (152 mg, 0.518 mmol) and PEt₃ (77 μL, 0.52 mmol) in diethyl ether (20 mL) was added a solution of LiBr (97 mg, 2.1 mmol) in THF (15 mL). The solution turned from orange to pink, and a white solid precipitated. After the mixture was stirred for 10 min, the volatile materials were completely removed under reduced pressure and the residue was extracted with a 1:1 mixture of pentane and diethyl ether (20 mL). This pink solution was filtered, and the filtrate was concentrated to ~10 mL. Vapor diffusion of hexamethyldisiloxane into this solution at room temperature gave large purple crystals of **1-Br** (149 mg, 73% yield); these were shown to be identical to the above sample by ¹H NMR spectroscopy.

Cp*Ni(PEt₃)Me (1-Me). To a solution of Cp*Ni(acac) (0.83 g, 2.8 mmol) and PEt₃ (0.41 mL, 2.8 mmol) in diethyl ether (60 mL) was added 3.7 mL of a 0.77 M diethyl ether solution of MeLi (2.8 mmol) at 0 °C. Upon mixing, the solution immediately changed color from red to greenish-brown and a gray precipitate formed. After the mixture was stirred at 0 °C for 4 h, the volatile materials were removed under reduced pressure and the residue was extracted with pentane (75 mL). The green solution was filtered, and the filtrate was concentrated to ~30 mL. Cooling to -80 °C afforded deep green plates. Concentration of the mother liquor provided an additional crop of crystals for a total yield of 0.75 g (2.3 mmol, 81% yield). Mp 88–89 °C. IR: 2722 (w), 2268 (w), 1431 (sh), 1421 (sh), 1359 (m), 1249 (m), 1161 (w), 1143 (s), 1063 (w), 1035 (s), 1023 (s), 999 (sh), 985 (w), 965 (w), 945 (w), 767 (s), 715 (s), 669 (w), 631 (m), 587 (w), 545 (w), 515 (m), 445 (m), 405 (w), 363 (m), 332 (w), 303 (w). ¹H NMR (C₆D₆): δ 1.80 (d, *J* = 0.8 Hz, 15H, C₅Me₅), 1.17 (d of q, *J* = 7.5, 7.5 Hz, 6H, CH₂CH₃), 0.84 (d of t, *J* = 15, 7.5 Hz, 9H, CH₂CH₃). ³¹P{¹H} NMR (C₆D₆): 34.92. EIMS: 326 (100, 100); 327 (19, 19); 328 (40, 40); 329 (9, 9); 330 (6, 6). Anal. Calcd for C₁₇H₃₃NiP: C, 62.4; H, 10.17. Found: C, 62.2; H, 10.74.

X-ray Crystal Structure Determinations. All single crystals were grown from concentrated pentane solutions at -30 °C, except **1-PEt₃**, for which the crystal was grown from a THF/Et₂O mixture at room temperature. The structures of **1-Br** and **1-Me** were performed on an Enraf-Nonius CAD4 diffractometer at the CHEXRAY facility at Berkeley; the general procedure used on this system has been described.² The other structure determinations below were performed on the SMART/CCD system at the CHEXRAY facility at Berkeley; the procedure used on this system has been described.²⁴ Details regarding the individual structure determinations may be found below, in Tables

1 and 2, or in the Supporting Information. Details of the structure of **1-NHTol** can be found in the accompanying paper.⁶

Cp*Ni(PEt₃)Br (1-Br). The set of three standard reflections used were (8, 1, 1); (6, -6, 1); (4, 6, -3). Intensity checks showed no appreciable decay over the course of the data collection; the crystal orientation matrix did not reorient during the data collection. An empirical absorption correction was applied to the data based on averaged azimuthal ψ scans, which showed a variation of $I_{\min}/I_{\max} = 0.75$ for the average relative intensity curve. Analysis of the data revealed no systematic absences, consistent with the space group *P4*. Redundant data were averaged, with 6 reflections rejected as "bad" (difference between equivalent reflections > 5 σ), yielding a final total of 1842 reflections.

The coordinates of the nickel and bromine atoms were determined by Patterson methods. All non-hydrogen atoms were refined anisotropically. A difference Fourier map revealed the positions of most of the hydrogen atoms. These atoms were placed in calculated positions. Prior to final refinement, two reflections were rejected as "bad" data due to their high values of $w \times \Delta^2$. The highest and lowest peaks in the final difference Fourier map had electron densities of 0.77 and -0.19 e⁻/Å³, respectively, and were associated with the nickel atom.

Cp*Ni(PEt₃)Me (1-Me). The original cell found and used for data collection was a nonprimitive doubled cell with C-centering. Upon transformation to a primitive cell, the dimensions and volume of the unit cell suggested tetragonal symmetry with 4 molecules in the unit cell. The set of three standard reflections used was (-2, 4, 5); (-7, -11, 2); (7, -11, -2). The intensities showed a slight linear intensity decay over the course of the data collection. The decay was expressed as a linear function and a correction was applied to the data, with a maximum correction of 1.8%. The crystal orientation matrix did not reorient during the data collection.

The DIFABS program was used for the empirical absorption correction; the maximum correction was 16%. Analysis of the systematic absences was consistent with a C-centered cell. After the cell transformation to the primitive cell, the 1814 remaining reflections showed no systematic absences, consistent with the space group *P4*.

The coordinates of Ni and P were determined by Patterson methods. Only the following atoms were refined anisotropically: the nickel, the Cp* ring carbons, and all non-hydrogen atoms related to the PEt₃ ligand. The methyl carbon was refined isotropically. The structure revealed a disorder of the Cp* ligand across a pseudo-mirror plane containing the nickel and phosphorus atoms, the methyl carbon, and C2 of the Cp* ligand. The methyl carbons of the Cp* ligand were modeled using a 2:1 occupancy ratio of two sites displaced circumferentially by ~0.5 Å in either direction from the predicted location of the methyl carbon (based on an idealized geometry for the Cp* ligand). A difference Fourier map revealed the positions of the methyl and PEt₃ hydrogen atoms. Only these atoms were placed in calculated positions. They were included in the structure factor calculations but not refined. The positions of the Cp* hydrogens were masked by the disorder, and hence were not included in the structure solution.

Prior to final refinement, eight reflections were rejected as "bad" data due to their high values of $w \times \Delta^2$. The highest and lowest peaks in the final difference Fourier map had electron densities of 0.97 and -0.39 e⁻/Å³, respectively, and were associated with the Cp* ring carbon atoms.

Cp*Ni(PEt₃)OTol (1-OTol). Inspection of the systematic absences indicated possible space groups *Pna2*₁ and *Pnma*; the choice of *Pna2*₁ was confirmed by successful solution and refinement of the structure. Of the 9312 reflections that were measured, 3555 were unique ($R_{\text{int}} = 5.3\%$); equivalent reflections were averaged, but Friedel pairs were not averaged. Attempts to refine the molecule in each enantiomorph form showed that the correct enantiomorph refined to a *R* value approximately 1.5% lower than the other enantiomorph. The non-hydrogen atoms were refined anisotropically. Most of the hydrogen atoms were located in a Fourier synthesis; however, they refined poorly, so they were included in F_{calc} calculations in idealized positions with isotropic *B*'s fixed at approximately 1.2 times the B_{eq} of the atom to which they were attached.

Cp*Ni(PEt₃)STol (1-STol). Inspection of the systematic absences uniquely indicated space group *P2*₁/*c*. Of the 19 211 reflections that were measured, 7002 were unique ($R_{\text{int}} = 3.9\%$); equivalent reflections

were averaged. The non-hydrogen atoms were refined anisotropically. The hydrogen atoms were located in Fourier syntheses and refined isotropically in the final stages of refinement, using fixed isotropic thermal parameters of ~ 1.2 times that of the atom to which they were attached.

Cp*Ni(PEt₃)CH₂Ph (1-Bn). Inspection of the systematic absences uniquely indicated space group $P2_1/c$. Of the 17 851 reflections that were measured, 6562 were unique ($R_{\text{int}} = 4.8\%$); equivalent reflections were averaged. The non-hydrogen atoms were refined anisotropically. The hydrogen atoms were located in Fourier syntheses and their positions were refined in the final stages of refinement, using fixed isotropic thermal parameters of ~ 1.2 times that of the atom to which they were attached.

Cp*Ni(PEt₃)H (1-H). Inspection of the systematic absences uniquely indicated space group $P2_1/c$. Of the 6994 reflections that were measured, 2584 were unique ($R_{\text{int}} = 2.7\%$); equivalent reflections were averaged. The non-hydrogen atoms were refined anisotropically. The hydrogen atoms were located in Fourier syntheses and their positions were refined isotropically in the final stages of refinement. The hydride hydrogen atom behaved well in refinement: electron density difference maps showed that this atom was not merely an artifact, and the reasonable bond distance and angles confirm the identification of this atom in the model.

Cp*Ni(PEt₃)OMe (1-OMe). Inspection of the systematic absences indicated possible space groups $P2/c$ and Pc ; selection of $P2/c$ was confirmed by successful solution and refinement of the structure. The non-hydrogen atoms were refined anisotropically. The hydrogen atoms were located in Fourier syntheses and their positions were refined in the final stages of refinement, using fixed isotropic thermal parameters of ~ 1.2 times that of the atom to which they were attached. Atom

C(17) has an unusual anisotropic "motion": removing this atom, refining, and replacing the atom caused the model to refine to the same minimum reproducibly.

Cp*Ni(PEt₃)₂⁺OTf⁻ (1-PEt₃). Inspection of the systematic absences indicated space group $P2_1/n$ (an alternate setting of $P2_1/c$). Of the 11 697 reflections that were measured, 4192 were unique ($R_{\text{int}} = 8.8\%$); equivalent reflections were averaged. The non-hydrogen atoms were refined anisotropically. A disorder model for the triflate group was pursued, but the populations refined to approximately 1:1, and the R value was substantially lower with a nondisorder model. The hydrogen atoms were located in Fourier syntheses but refined poorly, so they were included in F_{calc} calculations in idealized positions with isotropic B 's fixed at ~ 1.2 times the B_{eq} of the atom to which they were attached.

Acknowledgment. The authors thank Dr. F. J. Hollander for invaluable assistance in the determination of the crystal structures, as well as for helpful discussions and a thoughtful reading of the manuscript. Thanks are also due to the National Institutes of Health (grant no. GM-25459) for funding and to the National Science Foundation for a predoctoral fellowship for M.E.S.

Supporting Information Available: ORTEP diagrams of **1-H**, **1-OTol**, and **1-STol**, and tables of positional parameters, thermal parameters, and bond distances for all crystal structure determinations (28 pages). See any current masthead page for ordering and Internet access instructions.

JA971830O